medRxiv preprint doi: https://doi.org/10.1101/2024.03.26.24304802; this version posted May 4, 2024. The copyright holder for this preprint (which was not certified by peer review) is the author/funder, who has granted medRxiv a license to display the preprint in perpetuity. It is made available under a CC-BY 4.0 International license .

Simulated resections and RNS placement can optimize post-operative seizure outcomes when guided by fast ripple networks.

Shennan Aibel Weiss[1,2,3], Michael R. Sperling[4], Jerome Engel Jr[7,8,9,10,11]., Anli Liu[14,16], Itzhak Fried[8], Chengyuan Wu[5,6], Werner Doyle[15], Charles Mikell III[17], Sima Mofakham[17], Noriko Salamon[12], Myung Shin Sim[13], Anatol Bragin[7], Richard Staba[7]

1. Dept. of Neurology, State University of New York Downstate, Brooklyn, New York 11203, USA
2. Dept. of Physiology and Pharmacology, State University of New York Downstate, Brooklyn, New York 11203, USA
3. Dept. of Neurology, New York City Health + Hospitals/Kings County, Brooklyn, NY, 11203 USA
4. Dept. of Neurology, Thomas Jefferson University, Philadelphia, PA 19107, USA
5. Dept. of Neuroradiology, Thomas Jefferson University, Philadelphia, PA, 19107, USA
6. Dept. of Neurosurgery, Thomas Jefferson University, Philadelphia, PA 19107, USA
7. Dept. of Neurology, David Geffen School of Medicine at UCLA, Los Angeles, California 90095, USA
8. Dept. of Neurosurgery, David Geffen School of Medicine at UCLA, Los Angeles, California 90095, USA
9. Dept. of Neurobiology, David Geffen School of Medicine at UCLA, Los Angeles, California 90095, USA
10. Dept. of Psychiatry and Biobehavioral Sciences, David Geffen School of Medicine at UCLA, Los Angeles, California 90095, USA
11. Brain Research Institute, David Geffen School of Medicine at UCLA, Los Angeles, California 90095, USA
12. Dept. of Neuroradiology, David Geffen School of Medicine at UCLA, Los Angeles, California 90095, USA
13. Dept. of Medicine, David Geffen School of Medicine at UCLA, Los Angeles, California 90095, USA
14. Department of Neurology, NYU Grossman School of Medicine, New York, NY, 10016 USA
15. Department of Neurosurgery, NYU Grossman School of Medicine, New York, NY, 10016 USA
16. Neuroscience Institute, NYU Langone Medical Center, New York, NY, 10016 USA
17. Department of Neurosurgery, State University of New York Stony Brook, Stony Brook, New York 11790, USA

Corresponding author: Shennan Aibel Weiss shennanweiss@gmail.com

Total words: 3526

NOTE: This preprint reports new research that has not been certified by peer review and should not be used to guide clinical practice.

medRxiv preprint doi: https://doi.org/10.1101/2024.03.26.24304802; this version posted May 4, 2024. The copyright holder for this preprint
(which was not certified by peer review) is the author/funder, who has granted medRxiv a license to display the preprint in perpetuity.
It is made available under a CC-BY 4.0 International license .

Abstract (254 words)

In medication-resistant epilepsy, the objective of epilepsy surgery is to render a patient seizure free with a resection/ablation that is as small as possible to minimize morbidity. The standard of care in planning the margins of epilepsy surgery involves electroclinical delineation of the seizure onset zone (SOZ) in the epilepsy monitoring unit (EMU) by an expert epileptologist, and incorporation of neuroimaging findings from MRI, PET, SPECT, and MEG modalities. Resecting cortical tissue generating high-frequency oscillations (HFOs) has been investigated as a more efficacious alternative to targeting the SOZ. In this study, we used support vector machines (SVMs) to compare the resection volumes of actual resections, defined using the clinical standard of care, with virtual resections of fast ripple (FR 350-600 Hz) networks. Cross-validation of the SVM that labeled patients as seizure free or not seizure free using FR metrics as factors demonstrated an accuracy of 0.78. In all the patients rendered seizure free after surgery, we found that the virtual resection, defined using FR generator sites with highest rate and greatest autonomy, was larger than the actual resection. In the patients who experienced seizures after the actual resection, a virtual resection that included the SOZ and other FR generating regions rendered half of these patients virtually seizure free. We also examined patients implanted with the responsive neurostimulator system (RNS) and virtually targeted the RNS stimulation contacts proximal to sites generating FR. We used the simulations to investigate if the likelihood of a RNS super response (>90% seizure reduction) would be increased.

Key words:

Epilepsy surgery, neuromodulation, high-frequency oscillation, fast ripple, seizure onset zone, virtual resection

medRxiv preprint doi: https://doi.org/10.1101/2024.03.26.24304802; this version posted May 4, 2024. The copyright holder for this preprint (which was not certified by peer review) is the author/funder, who has granted medRxiv a license to display the preprint in perpetuity. It is made available under a CC-BY 4.0 International license .

Introduction (960 words)

The standard of care for planning an efficacious epilepsy surgery, with minimal morbidity, is electroclinical delineation of the seizure onset zone (SOZ) in the epilepsy monitoring unit by an expert epileptologist, integrated with neuroimaging findings from MRI, PET, SPECT, and MEG modalities[1] and consideration of seizure semiology. Even if the SOZ is sufficiently sampled by the stereo EEG (SEEG) implant, resection of the SOZ does not always correlate with seizure outcome[2–7], and thus a considerable percentage of patients that undergo epilepsy surgery are not rendered seizure free[8–10]. This is especially true for patients with certain epilepsy etiologies such as non-lesional frontal lobe epilepsy[8]. However, utilizing the rates (events/min) of interictal high-frequency oscillations (HFOs: 80-600 Hz) recorded during non-REM sleep could be an alternative to the clinical standard of care of delineating the boundaries of the SOZ[11,12].

In the current study, we focused on a subpopulation of HFOs known as fast ripples (200-600 Hz, FR). FR are brief (8-50 ms) bursts of oscillatory activity that are, in most context, pathological[13–16]. Analyzing hours of sleep improves the accuracy of localizing epileptogenic regions[12]. In retrospective studies, resecting 60% of FR events (i.e., FR resection ratio [RR]) had a 70-80% accuracy for predicting seizure freedom[12]. A challenge to utilizing FR prospectively to plan a resection is that ratio measures, such as the FR RR, do not specify the precise portion of the FR-generating sites that need to be resected. As an alternative approach, we utilized spatial and temporal FR graph theoretical metrics to generate objective solutions to help define the resection margins. These same metrics were then used as factors to train and test a support vector machine (SVM) that predicts whether the actual and/or simulated resection boundaries produces a seizure free outcome.

The first factor used in the SVM is the FR RR[12] and the second factor is a novel measure of the residual FR-generating territory following a resection. This measure is calculated using graph theoretical analysis[17] and is termed the “rate-distance radius resected difference” or RDRRD[18]. For simplicity, we refer to the RDRRD as spatial FRnet. We previously reported that Spatial FRnet classified post-operative seizure-free patients more accurately than the FR RR[19].

The third and fourth factor of the SVM were based on FR temporal correlations that can be utilized to identify the most important nodes in the FR network for defining the virtual resections. We utilized FR onset times to calculate FR mutual information (MI) between FR nodes (*i.e.,* SEEG contacts). The FR MI value weighted the edges of the FR network. We then used this FR MI temporal correlational network to derive global and local graph measures. This strategy was based on our past work established that: 1) a FR MI network with a longer path length (□) correlated with a failure to improve after surgery[18]; and 2) a failure to resect nodes generating FR at high rates and desynchronously (*i.e.,* autonomously) with other nodes correlated with a failure to achieve post-operative seizure freedom[19]. Specifically, the third and fourth factor used for the SVM are: a) the path length resection ratio (□RR), herein referred to as temporal FRnet-A; and b) unresected mean local efficiency (urmLE)[19]**,** herein referred to as temporal FRnet-B.

The spatial and temporal FR graph theoretical measures were used to iteratively identify the most important SEEG electrode contacts (i.e., sites) generating FR at the highest rate and most autonomously (i.e., FR events that occur in one electrode contact but not synchronously in other contacts) and thereby plan a virtual resection. In patients who were rendered seizure free after epilepsy surgery, we assessed whether a virtual resection associated with seizure free outcome per the SVM would be smaller or larger than the resection guided by the clinical standard of care. We also examined if the virtual resection targeting FR

medRxiv preprint doi: https://doi.org/10.1101/2024.03.26.24304802; this version posted May 4, 2024. The copyright holder for this preprint (which was not certified by peer review) is the author/funder, who has granted medRxiv a license to display the preprint in perpetuity. It is made available under a CC-BY 4.0 International license .

sites would encompass a greater extent of the SOZ or spike ripple (80-200 Hz) sites[20] than the traditional standard of care resection.

Additionally, we examined patients implanted with the responsive neurostimulation (RNS) device and asked if alternate placement of the RNS stimulation contacts at sites generating FR at high rates would predict a better seizure outcome. To approximate the brain regions that were maximally stimulated by the actual and virtual RNS placements, we defined the pre-implant SEEG electrode stimulated contacts as within a radius of <1.5 cm of the eight RNS contacts (i.e., two leads of either a four-contact depth or subdural strip)[21]. Our justification for using this method was that RNS stimulation intensities typically ranged from ~1-3 mAmps and monopolar stimulation would produce an electric field of ~2-4 mV/mm at 1.5 cm away from the stimulation source[22]. Since electric field strengths of at least 2-4 mV/mm can induce spike field coherence[23,24], and smaller fields at distances greater than 1.5 cm may only influence spike timing[25]. We next calculated the SOZ stimulation ratio (SR), FR SR, and the FR stimulated global efficiency (SGe), herein described as RNS temporal FRnet[26] using the boundaries of the calculated stimulated brain regions. Lastly, we asked if these values differed in patients with a super responder (>90% seizure reduction) clinical outcome[26].

Although the number of patients in our resection/ablation and RNS cohort were relatively small, we approximated statistical power calculations that could be utilized to plan a prospective randomized controlled trial. We based these approximations on the accuracy of the SVM and the number of non-seizure free patients who could be rendered virtually seizure free by inclusion of nodes from the virtual FR resections. A similar approach was utilized to examine the RNS patient cohort based on measures of RNS temporal FRnet resulting from virtual placement of the RNS stimulation contacts.

Methods (1035 words)

Patients

Consecutive recordings selected from 14 patients who underwent intracranial monitoring with depth electrodes between 2014 and 2018 at the University of California Los Angeles (UCLA) and from 19 patients at the Thomas Jefferson University (TJU) in 2016–2018 for the purpose of localization of the SOZ. Data collection was planned before the study was conceptualized. Among these 28 patients, 18 underwent resections and ablations and 10 were implanted with RNS. Inclusion criteria for this study included pre-surgical MRI for MRI-guided stereotactic electrode implantation, as well as a post-implant CT scan to localize the electrodes, and stereo EEG recordings during non-rapid eye movement (REM) sleep at a 2 kHz sampling rate. Patients were excluded if: 1) no resection/ablation or RNS placement was performed; 2) a post-resection/ablation MRI or a post-RNS implant CT was not obtained; 3) no adequate post-operative clinical follow up; 4) A failure to record at least ten minutes of artifact free iEEG during non-REM sleep; and 5) graph theoretical analysis indicated incomplete or poor spatial sampling[19]. All patients provided verbal and written consent prior to participating in this research, which was approved by the UCLA and TJU institutional review boards. Eligible patients were identified through queries of pre-existing clinical databases. The epileptologist defined SOZ was aggregated across all these seizures during the entire iEEG evaluation for each patient[18].

Neuroimaging

Using an in-house pipeline (https://github.com/pennmem/neurorad_pipeline), T1- pre-implant and post-resection MRIs were obtained for each patient. Post-implantation SEEG and RNS CT

medRxiv preprint doi: https://doi.org/10.1101/2024.03.26.24304802; this version posted May 4, 2024. The copyright holder for this preprint (which was not certified by peer review) is the author/funder, who has granted medRxiv a license to display the preprint in perpetuity. It is made available under a CC-BY 4.0 International license .

scans were then co-registered and normalized with the MRIs using Advanced Neuroimaging Tools (ANTs)[27] with neuroradiologist supervision. The position of each electrode contact in the post-SEEG implant CT and post-RNS placement CT was localized to normalized MNI coordinates and the Desikan-Killiany atlas[28]. Identification of the named electrode contacts in the resection cavity was performed manually in itk-SNAP.

EEG recordings and HFO detection

Clinical iEEG (0.1–600 Hz; 2000 samples per second) was recorded from 8 to 16 depth electrodes, each with 7–15 contacts, using a Nihon-Kohden 256-channel JE-120 long-term monitoring system (Nihon-Kohden America, Foothill Ranch, CA, USA), for each patient. A larger number of electrodes with more contacts were implanted at TJU. For the recordings performed at UCLA. the reference signal used for was a scalp electrode position at Fz. The reference signal used for the TJU recordings was an electrode in the white matter. HFOs and sharp-spikes were detected in the non-REM sleep iEEG using previously published methods (https://github.com/shenweiss)[29–33] implemented in Matlab (Mathworks, Natick, MA, USA) from 10-60 minutes, per patient[19]. All other programming, including the virtual resection simulations, was done using Matlab. Following automatic detection of HFO and sharp-spikes, false detections of clear muscle and mechanical artifact were deleted by visual review in Micromed Brainquick (Venice, Italy).

Fast ripple derived. predictors of post-resection/ablation seizure outcome

The SOZ, FR (fast ripple on oscillation > 350 Hz, and all fast ripple on spike)[18,19,34] and RonS resection ratio (RR) were derived as the number of SOZ contacts, FR or RonS events on removed channels divided by total number of SOZ contacts or events on all channels. All graph theoretical measures were calculated using the Brain Connectivity Toolbox (https://sites.google.com/site/bctnet/)[35]. The adjacency matrix for the spatial FRnet (FR rate–distance radius resected difference RDRRD) was calculated by the average rate (/min) of the events recorded by two respective nodes multiplied by the Euclidian distance (mm) between these nodes. The adjacency matrix for the mutual information (MI) networks were calculated using FR event 'spike trains' defined by the onset times of each event and then calculating MI between nodes using the adaptive partition using inter-spike intervals MI estimator.[36] Using these adjacency matrices, and their inverses, the temporal FRnet A and B were calculated[19]. Support vector machines (SVM) were trained on the actual measures: 1) FR RR; 2) spatial FRnet; 3) temporal FRnet-A,B. The SVM was trained after normalizing the data and using a Radial Basis Function kernel that is automatically scaled to reduce the effect of outliers on SVM training[18].

Virtual Resections and Outcome Prediction

The initial virtual resection volume was determined by defining all the graph nodes (i.e., contacts) with a FR rate > 1/minute as a candidate set and finding the node with the smallest local efficiency (LE) as the candidate node in the candidate set. If no contacts exhibited a FR rate > 1 minute, or no such nodes remained in the candidate set, all nodes were included in the candidate set and the candidate node was selected as the node with the highest FR rate. The candidate node served as the center of the sphere of the virtual resection(s). A resection sphere with a 1 cm radius was initially simulated, centered on this initial candidate node, and all nodes falling within this sphere were included in the virtual resected set after excluding contralateral contacts. For all the nodes in the virtual resected set, the SOZ RR, RonS RR, FR RR, spatial

medRxiv preprint doi: https://doi.org/10.1101/2024.03.26.24304802; this version posted May 4, 2024. The copyright holder for this preprint
(which was not certified by peer review) is the author/funder, who has granted medRxiv a license to display the preprint in perpetuity.
It is made available under a CC-BY 4.0 International license .

FRnet, and temporal FRnet-A,B were calculated. Additionally, we quantified the proportion of overlapping and non-overlapping nodes in the virtual resected set and the set of nodes in the actual resection. Then, in the second iteration of the simulation, the node with second lowest LE, or second highest FR rate, was included in the resected set. The radius between the initial node and this second resected node, with an additional 1 cm buffer, was used to calculate a second sphere and define the new resected set. Iteration of the simulation continued through all the candidate nodes in the candidate set with an incrementally increasing, but not decreasing, radius. For each iteration of the simulation, the SVM predicted whether the outcome was seizure free.

Virtual RNS stimulation lead placement

The 10 patients with RNS placement were subdivided into those with bilateral and unilateral placement of the RNS stimulation leads. For patients with bilateral placement, we defined two sets of nodes, for each hemisphere, with the highest FR rate. For patients with ipsilateral placement of the two stimulation leads, we defined two sets as ipsilateral contacts with the highest FR rate. We found the corresponding two sets of four "stimulation contacts" that generated FR at the highest rates. We then calculated the corresponding SOZ stimulation ratio, FR stimulation rate, and RNS temporal FRnet[21].

Results (1188 words)

Patient characteristics

The study cohort for patients that underwent resections consisted of 23 patients, 12 males and 11 females, and excluded 36 other patients (see methods)[19]. The patients had diverse etiologies with 6 of the 23 with normal MRI findings[19]. The SOZ were non-exclusively localized to the mesial temporal lobe and cingulate cortex in 14 patients, lateral temporal lobe in 7, frontal lobe in 9, and parietal lobe in 3. Among these 23 patients, five patients had multilobar SOZs. Ten patients received an anterior temporal lobectomy and 2 patients laser ablation. In 6 of the 23 patients, the operation was a surgical revision. The post-operative seizure outcome was seizure free in 10 and non-seizure free in 13. Mean time at last follow up was 31.45 ± 3.1 months (standard error of the mean). The patient characteristics of the RNS patients are described in a previous study[21], and among these ten patients 7 were intermediate responders and 3 were super responders[26]. Further details regarding the patients included in this study can be found in our prior publications[19,21].

Spatial sampling limitations

Among the 23 patients who underwent resection our results from three of the non-seizure free patients suggested incomplete SEEG spatial sampling. We defined incomplete spatial sampling as a failure to achieve seizure freedom despite resection of the entire FR network. We also found that one seizure free and one non-seizure patient with poor spatial sampling. In these patients, FR networks could not be characterized, and no electrode contact generated FR on spikes at a rate of > 1/min[19]. Since these five patients could confound SVM training they were excluded from the study.

Support vector machine training

medRxiv preprint doi: https://doi.org/10.1101/2024.03.26.24304802; this version posted May 4, 2024. The copyright holder for this preprint (which was not certified by peer review) is the author/funder, who has granted medRxiv a license to display the preprint in perpetuity. It is made available under a CC-BY 4.0 International license .

SVM training was performed using the FR RR, and spatial- and temporal-FRnet measures of the remaining 18 patients, as well as their seizure outcome. A 100-fold cross validation of the trained SVM demonstrated a loss of 0.22 equivalent to an accuracy of 0.78. We then tested the trained SVM on FR RR, and spatial- and temporal-FRnet measures derived from virtual resections in individual patients.

Virtual resections

In the nine patients who had a seizure free outcome, the virtual resections associated with seizure freedom mostly included all of the SOZ (mean SOZ RR = 0.87 ± 0.07) and most regions with spike ripples (spike ripples RR = 0.76 ± 0.08) (Table 1, Figure 1,2). The virtual resection encompassed the actual resection contacts (86.7 ± 6.7% actual resection included in virtual resection) and included other unresected contacts too. Across the nine patients, 49.4 ± 8.0% of the contacts in the virtual resection were not actually resected. Results from the simulation imply the resection size informed by the spatial- and temporal-FRnet measures that produced seizure freedom is larger than the actual resection determined by the clinical standard of care that resulted in seizure freedom.

In the nine patients who were not seizure free after surgery, the simulation predicted five patients could be rendered seizure free by virtual resections (Table 2, Figure 1,2). The virtual resection that rendered these five patients seizure free encompassed most of the SOZ (95.6 ± 4.5%) and regions with spike ripples (87.1% ± 3.0%), and overall, the virtual resections partially encompassed the contacts of the real resections (65.5 ± 19.3%). However, the virtual resection also included a substantial proportion of unresected contacts (69.6 ± 9.6%). Exceptions included patient IO015 who did not actually undergo a resection of the SOZ, and patient 4110 in which the virtual resection did not encompass most of the SOZ. In the remaining four patients who were not seizure free after surgery or after virtual resection (Table 2, Figure 1,2), either the spatial FRnet value remained elevated and/or the temporal FRnet-B was relatively closer to zero.

Power calculations for use of virtual resections in a randomized controlled clinical trial

The ultimate goals in the surgical and RNS treatment of medication-resistant epilepsy are the elimination or complete control of seizures with minimal morbidity. Towards these goals results from our simulations could be used in power calculations to design a randomized controlled trial (RCT) to compare two approaches to epilepsy surgery: a control arm comprised of the standard resection based on the clinical standard of care, and an active arm that contains an innovative approach that uses the combination of standard resection and results from SVM model. The active arm would use the SVM model to predict whether a standard SOZ resection will produce a seizure free outcome. If the SVM model predicts that a standard resection will not produce seizure freedom, then the virtual resection targeting sites in the spatial- and temporal-FRnet could be used to amend the original surgical plan. The decision to proceed with the modified resection plan would be contingent on the agreement from the patient and the surgeon.

In the current study using our SVM model and power calculations, a sample size of 150 patients in each arm will provide 80% power to detect a difference of 0.15 in achieving seizure freedom rate between the two arms. This is based on the assumption that the control arm exhibits a 60% seizure freedom and the active arm, benefitting from SVM-guided amendments, shows a significantly higher seizure freedom of 75%. The difference in seizure freedom between the approaches are consistent with our preliminary results demonstrating an SVM classification

medRxiv preprint doi: https://doi.org/10.1101/2024.03.26.24304802; this version posted May 4, 2024. The copyright holder for this preprint (which was not certified by peer review) is the author/funder, who has granted medRxiv a license to display the preprint in perpetuity. It is made available under a CC-BY 4.0 International license .

accuracy near 0.8 and virtual resections based on spatial- and temporal FRnet measures that predicted a seizure free outcome in five of nine subjects. Two-sided Z-test with unpooled variance was used at a significance level of 0.05, to rigorously evaluate the efficacy of incorporating FR net analyses into surgical planning for epilepsy treatment. Anticipating a differential dropout rate because of 1) an inability to fully resect the SOZ due to overlap with eloquent cortex; 2) the refusal by patients and or physician for amended resections; and 3) patients who are lost to follow up with approximately 25% expected in the active arm compared 10% in the control arm. To account for these participant losses the RCT would need to enroll 200 and 167 subjects in the active arm and control arm, respectively, to maintain the power to detect differences in seizure freedom.

RNS simulations

Unlike the virtual resection experiments, we did not train a SVM to discriminate RNS super responders from RNS intermediate responders because of our small sample size of 10 patients. In our prior study, we found that among these 10 RNS patients the RNS temporal FRnet value was smaller only in the three RNS super responder patients[21]. We found that by virtually stimulating the nodes with the highest FR rates, the RNS temporal FRnet was substantially smaller in the three super-responder patients but also in two intermediate responder patients (Figure 3). This suggests that targeting RNS stimulation to highly active FR generating tissue may increase the number of super responders.

To retrospectively investigate the possible efficacy of RNS simulations in a larger cohort that could then be used to plan a prospective clinical trial, based on this preliminary simulation, enrolling a total of 20 patients, divided equally into two groups: one active arm receiving RNS placement informed by our novel data analysis techniques, and one control arm subjected to standard RNS placement procedures. This sample size will achieve 80% power to detect a difference 0.5 between the group proportions of super responders. The proportion of super responders in the control arm is assumed to be 0.3. The test statistic used is the two-sided Z-Test with unpooled variance at 0.05 significance level. A critical goal of this aim is to accurately estimate the effect size of our intervention, which is pivotal for the planning of future, more extensive research.

Discussion (793 words)

In the current study, we trained a SVM to label patients as seizure free or not seizure free using four FR metrics as factors. The trained SVM was then utilized to classify a virtual resection based on spatial- and temporal-FRnet measures as seizure free or not. Two limitations of our approach are: 1) the patients used for SVM training were also used for SVM testing and thus the SVM may have been overtrained; 2) The seizure free and non-seizure free subjects were distinguished based on their actual clinical post-operative seizure outcome rather than the outcome predicted by the SVM based on the clinical standard of care resection. Since the cross-validated SVM exhibited an accuracy of only 0.78, the outcome predictions based on the FR virtual resections should be interpreted with caution.

Despite these limitations, the most pertinent finding of our study pertains to a comparison between the extent of the actual resection based on clinical standard of care and the virtual resection using spatial- and temporal-FRnet measures in surgical patients with a seizure free outcome. We found that the actual resection was smaller in size (i.e., number of electrode contacts resected) than the virtual resection from the SVM that predicted seizure freedom. It is

medRxiv preprint doi: https://doi.org/10.1101/2024.03.26.24304802; this version posted May 4, 2024. The copyright holder for this preprint (which was not certified by peer review) is the author/funder, who has granted medRxiv a license to display the preprint in perpetuity. It is made available under a CC-BY 4.0 International license .

unclear if resection margins defined by other HFO subtypes would also result in more spatially expansive resections as compared to the clinical standard of care. Notably, in surgical patients with a seizure free outcome, the virtual FR resection included most contacts designated as the SOZ and contacts containing a high rate of spike ripples[20,37,38].

In 5 of the 9 patients not seizure free after surgery, the SVM virtual resection removing spatial- and temporal-FRnet measures could predict a seizure free outcome. Future work can identify the most suitable methodology to amend the resection using the clinical standard of care combined with the iterative addition of high-rate and autonomous FR sites outside the resection boundaries. This strategy involves utilizing the SVM at each iteration to classify the amended resection as seizure free or not. We report that this is feasible in most of the patients who were not seizure free. However, we identified two subjects in which the actual resection boundaries did not overlap with FR virtual resection boundaries. In such patients, amending the standard of care resection with FR generating sites outside the resection boundaries may not be straight forward. Additionally, the resection boundaries defined by the virtual resection do not consider regions of eloquent cortex that cannot be excised.

The power calculations indicate our methods described herein could be utilized for a RCT to improve resective epilepsy surgery outcomes. A larger retrospective study could be used to better train and test the LRM using two distinct cohorts. The success of this clinical trial is also dependent on the LRM accuracy labeling seizure-freedom in the test cohort. A larger retrospective study would also identify the ideal inclusion and exclusion criteria for the clinical trial.

With respect to the patients in this study implanted with an RNS system, we used virtual placements of the RNS stimulating contacts to derive RNS temporal FRnet values that may correlate with super-responder outcome. This preliminary result in a very small cohort of patients should be interpreted cautiously because super-responder outcome be dependent on targeting both the SOZ and FR generating sites[39]. We plan on further examining whether alternative virtual RNS placements can be used to predict RNS super responders by training and testing a SVM that labels RNS super responders using SOZ stimulation ratio, FR stimulation ratio, and RNS temporal FRnet as factors in a test set of RNS patients.

In summary, our results examining patients who underwent resection and ablations indicate that the resection determined by the clinical standard of care are smaller in scope than resection of autonomous, high-rate FR sites. A novel aspect of this study is that machine learning utilizing FR metrics could accurately predict if resection based on the clinical standard of care would produce a seizure free outcome. In cases of not seizure free, the resection boundaries could be amended to include the autonomous, high-rate FR sites outside the resection margins. We also present limited results that a similar approach can be utilized for improving the efficacy of RNS. The rationale for utilizing our spatial and temporal FRnet measures in the SVM is that FR can promote the generation of inter-ictal discharges[38,40] and seizures[41,42]. Moreover, FR propagate within[43] and outside[40] the SOZ. Thus, FR may be the substrate of an epileptic network that extends beyond just the SOZ and includes nodes in the non-SOZ that are necessary and sufficient for seizure generation[18].

References

1. Rosenow, F. & Lüders, H. Presurgical evaluation of epilepsy. *Brain* **124**, 1683–1700 (2001).

medRxiv preprint doi: https://doi.org/10.1101/2024.03.26.24304802; this version posted May 4, 2024. The copyright holder for this preprint
(which was not certified by peer review) is the author/funder, who has granted medRxiv a license to display the preprint in perpetuity.
It is made available under a CC-BY 4.0 International license .

2. Jacobs, J. *et al.* High-frequency electroencephalographic oscillations correlate with outcome of epilepsy surgery. *Ann Neurol* **67**, 209–220 (2010).

3. Akiyama, T. *et al.* Focal resection of fast ripples on extraoperative intracranial EEG improves seizure outcome in pediatric epilepsy. *Epilepsia* **52**, 1802–1811 (2011).

4. Weiss, S. A. *et al.* Seizure localization using ictal phase-locked high gamma. *Neurology* **84**, 2320–2328 (2015).

5. Li, A. *et al.* Neural fragility as an EEG marker of the seizure onset zone. *Nat Neurosci* 1–10 (2021) doi:10.1038/s41593-021-00901-w.

6. Khan, M. *et al.* Proportion of resected seizure onset zone contacts in pediatric stereo-EEG-guided resective surgery does not correlate with outcome. *Clin Neurophysiol* **138**, 18–24 (2022).

7. Lin, J. *et al.* High frequency oscillation network dynamics predict outcome in non-palliative epilepsy surgery. *Brain Commun.* **6**, fcae032 (2024).

8. Téllez-Zenteno, J. F., Dhar, R. & Wiebe, S. Long-term seizure outcomes following epilepsy surgery: a systematic review and meta-analysis. *Brain* **128**, 1188–1198 (2005).

9. Engel, J. *et al.* Early Surgical Therapy for Drug-Resistant Temporal Lobe Epilepsy: A Randomized Trial. *Jama* **307**, 922–930 (2012).

10. Spencer, D. D., Gerrard, J. L. & Zaveri, H. P. The roles of surgery and technology in understanding focal epilepsy and its comorbidities. *Lancet Neurology* **17**, 373–382 (2018).

11. Bragin, A., Wilson, C. L. & Engel, J. Chronic Epileptogenesis Requires Development of a Network of Pathologically Interconnected Neuron Clusters: A Hypothesis. *Epilepsia* **41**, S144–S152 (2000).

12. Bragin, A., Mody, I., Wilson, C. L. & Engel, J. Local Generation of Fast Ripples in Epileptic Brain. *J Neurosci* **22**, 2012–2021 (2002).

13. Li, L. *et al.* Spatial and temporal profile of high-frequency oscillations in posttraumatic epileptogenesis. *Neurobiol Dis* **161**, 105544 (2021).

14. Weiss, S. A. *et al.* Pathological neurons generate ripples at the UP-DOWN transition disrupting information transfer. (2023) doi:10.1101/2023.08.01.23293365.

15. Nevalainen, P. *et al.* Association of fast ripples on intracranial EEG and outcomes after epilepsy surgery. *Neurology* **95**, e2235–e2245 (2020).

16. Bullmore, E. & Sporns, O. Complex brain networks: graph theoretical analysis of structural and functional systems. *Nat Rev Neurosci* **10**, 186–198 (2009).

17. Weiss, S. A. *et al.* Graph theoretical measures of fast ripples support the epileptic network hypothesis. *Brain Commun* (2022) doi:10.1093/braincomms/fcac101.

medRxiv preprint doi: https://doi.org/10.1101/2024.03.26.24304802; this version posted May 4, 2024. The copyright holder for this preprint
(which was not certified by peer review) is the author/funder, who has granted medRxiv a license to display the preprint in perpetuity.
It is made available under a CC-BY 4.0 International license .

18. Weiss, S. A. *et al.* Graph theoretical measures of fast ripple networks improve the accuracy of post-operative seizure outcome prediction. *Sci. Rep.* **13**, 367 (2023).

19. Fedele, T. *et al.* Resection of high frequency oscillations predicts seizure outcome in the individual patient. *Sci Rep-uk* **7**, 13836 (2017).

20. Dimakopoulos, V. *et al.* Blinded study: prospectively defined high-frequency oscillations predict seizure outcome in individual patients. *Brain Commun* **3**, fcab209 (2020).

21. Weiss, S. A. *et al.* Stimulation better targets fast-ripple generating networks in super responders to the responsive neurostimulator system. *Epilepsia* (2023) doi:10.1111/epi.17582.

22. Plonsey, R. & Barr, R. C. *Bioelectricity A Quantitative Approach*. (Kluwer Academic/Plenum Publishers, 2000).

23. Ozen, S. *et al.* Transcranial electric stimulation entrains cortical neuronal populations in rats. *J Neurosci Official J Soc Neurosci* **30**, 11476–85 (2010).

24. Anastassiou, C. A., Perin, R., Markram, H. & Koch, C. Ephaptic coupling of cortical neurons. *Nat Neurosci* **14**, 217–223 (2011).

25. Radman, T., Su, Y., An, J. H., Parra, L. C. & Bikson, M. Spike Timing Amplifies the Effect of Electric Fields on Neurons: Implications for Endogenous Field Effects. *J Neurosci* **27**, 3030–3036 (2007).

26. Khambhati, A. N., Shafi, A., Rao, V. R. & Chang, E. F. Long-term brain network reorganization predicts responsive neurostimulation outcomes for focal epilepsy. *Sci Transl Med* **13**, eabf6588 (2021).

27. Avants, B. B., Epstein, C. L., Grossman, M. & Gee, J. C. Symmetric diffeomorphic image registration with cross-correlation: Evaluating automated labeling of elderly and neurodegenerative brain. *Med Image Anal* **12**, 26–41 (2008).

28. Desikan, R. S. *et al.* An automated labeling system for subdividing the human cerebral cortex on MRI scans into gyral based regions of interest. *Neuroimage* **31**, 968–980 (2006).

29. Waldman, Z. J. *et al.* A method for the topographical identification and quantification of high frequency oscillations in intracranial electroencephalography recordings. *Clin Neurophysiol* **129**, 308–318 (2018).

30. Weiss, S. A. *et al.* Accuracy of high-frequency oscillations recorded intraoperatively for classification of epileptogenic regions. *Sci Rep-uk* **11**, 21388 (2021).

31. Song, I. *et al.* Bimodal coupling of ripples and slower oscillations during sleep in patients with focal epilepsy. *Epilepsia* **58**, 1972–1984 (2017).

32. Shimamoto, S. *et al.* Utilization of independent component analysis for accurate pathological ripple detection in intracranial EEG recordings recorded extra- and intra-operatively. *Clin Neurophysiol* **129**, 296–307 (2018).

medRxiv preprint doi: https://doi.org/10.1101/2024.03.26.24304802; this version posted May 4, 2024. The copyright holder for this preprint
(which was not certified by peer review) is the author/funder, who has granted medRxiv a license to display the preprint in perpetuity.
It is made available under a CC-BY 4.0 International license .

33. Weiss, S. A. *et al.* Visually validated semi-automatic high-frequency oscillation detection aides the delineation of epileptogenic regions during intra-operative electrocorticography. *Clin Neurophysiol* **129**, 2089–2098 (2018).

34. Weiss, S. A. *et al.* Pathological neurons generate ripples at the UP-DOWN transition disrupting information transfer. *Epilepsia* **65**, 362–377 (2023).

35. Rubinov, M. & Sporns, O. Complex network measures of brain connectivity: Uses and interpretations. *Neuroimage* **52**, 1059–1069 (2010).

36. Gribkova, E. D., Ibrahim, B. A. & Llano, D. A. A novel mutual information estimator to measure spike train correlations in a model thalamocortical network. *J Neurophysiol* **120**, 2730–2744 (2018).

37. Guth, T. A. *et al.* Interictal spikes with and without high-frequency oscillation have different single-neuron correlates. *Brain* (2021) doi:10.1093/brain/awab288.

38. Weiss, S. A. *et al.* Fast ripples reflect increased excitability that primes epileptiform spikes. *Brain Commun.* fcad242 (2023) doi:10.1093/braincomms/fcad242.

39. Shi, W. *et al.* Spike ripples localize the epileptogenic zone best: an international intracranial study. *Brain* awae037 (2024) doi:10.1093/brain/awae037.

40. Miles, R. & Wong, R. K. S. Single neurones can initiate synchronized population discharge in the hippocampus. *Nature* **306**, 371–373 (1983).

41. Prince, D. A. & Wilder, B. J. Control Mechanisms in Cortical Epileptogenic Foci*: Surround Inhibition. *Arch Neurol-chicago* **16**, 194–202 (1967).

42. Trevelyan, A. J., Sussillo, D. & Yuste, R. Feedforward Inhibition Contributes to the Control of Epileptiform Propagation Speed. *J Neurosci* **27**, 3383–3387 (2007).

43. Trevelyan, A. J., Sussillo, D., Watson, B. O. & Yuste, R. Modular Propagation of Epileptiform Activity: Evidence for an Inhibitory Veto in Neocortex. *J Neurosci* **26**, 12447–12455 (2006).

44. Weiss, S. A. *et al.* Delta oscillation coupled propagating fast ripples precede epileptiform discharges in patients with focal epilepsy. *Neurobiol Dis* 105928 (2022) doi:10.1016/j.nbd.2022.105928.

45. Schevon, C. A. *et al.* Evidence of an inhibitory restraint of seizure activity in humans. *Nat Commun* **3**, 1060 (2012).

46. Weiss, S. A. *et al.* Ictal high frequency oscillations distinguish two types of seizure territories in humans. *Brain* **136**, 3796–3808 (2013).

47. Schlafly, E. D. *et al.* Multiple sources of fast traveling waves during human seizures: resolving a controversy. *J Neurosci Official J Soc Neurosci* **42**, 6966–6982 (2022).

medRxiv preprint doi: https://doi.org/10.1101/2024.03.26.24304802; this version posted May 4, 2024. The copyright holder for this preprint (which was not certified by peer review) is the author/funder, who has granted medRxiv a license to display the preprint in perpetuity. It is made available under a CC-BY 4.0 International license .

48. Weiss, S. A. Chloride ion dysregulation in epileptogenic neuronal networks. *Neurobiol Dis* **177**, 106000 (2023).

Funding statement:
This work was fully supported by the National Institute of Health K23 NS094633, a Junior Investigator Award from the American Epilepsy Society (S.A.W.), R01 NS106957(R.J.S.) and R01 NS033310 (J.E.).

Author Contributions

Credit author statement: **Shennan Aibel Weiss:** conceptualization, methodology, software, investigation, resources, writing – original draft, writing – review & editing, funding acquisition. **Anli Liu**: investigation, writing – review & editing. **Werner Doyle:** investigation, writing – review & editing. **Charles Mikell III**: investigation, writing – review & editing. **Sima Mofakham**: investigation, writing – review & editing. **Noriko Salamon**: investigation, writing – review & editing. **Myung Shin Sim:** conceptualization, methodology, software, investigation, resources, writing – original draft, writing – review & editing, funding acquisition. **Itzhak Fried:** resources. **Chengyuan Wu:** resources. **Ashwini Sharan:** resources. **Jerome Engel:** writing – review & editing, funding acquisition. **Richard Staba:** investigation, writing – review & editing, funding acquisition. **Michael R. Sperling:** investigation, writing – review & editing, funding acquisition.

Data availability

The datasets generated during and/or analysed during the current study are available from the corresponding author on reasonable request.

Disclosures Statement: S.A.W. M.R.S has received compensation for speaking at continuing medical education (CME) programs from Medscape, Projects for Knowledge, International Medical Press, and Eisai. He has consulted for Medtronic, Neurelis, and Johnson & Johnson. He has received research support from Eisai, Medtronic, Neurelis, SK Life Science, Takeda, Xenon, Cerevel, UCB Pharma, Janssen, and Engage Pharmaceuticals. He has received royalties from Oxford University Press and Cambridge University Press.

Acknowledgements

We would also like to thank Christina Louise George Trust and the Resnick Family Foundation.

Tables

medRxiv preprint doi: https://doi.org/10.1101/2024.03.26.24304802; this version posted May 4, 2024. The copyright holder for this preprint (which was not certified by peer review) is the author/funder, who has granted medRxiv a license to display the preprint in perpetuity. It is made available under a CC-BY 4.0 International license .

Table 1: Virtual resection metrics at which patients actually rendered seizure free by surgery were predicted to be rendered seizure free by the virtual resection. Abbreviations: SOZ: seizure onset zone; sim:simulation; RR:resection ration; FR; fast ripple: FRnet: FR network graph theoretical measure; percent_r: percent of the nodes in resection cavity included in virtual resection set; novel_r: percent of nodes in the resection set that were not in the resection cavity.

Patient	sim. Radius	SOZ RR	Spike ripple RR	FRRR	spatial FRnet	temporal FRnet-A	temporal FRnet-B	percent_r	novel_r
1) 466	45.907	1.000	0.593	0.459	1.869	0.874	0.539	1.000	0.548
2) 477	18.565	1.000	0.880	0.845	3.561	3.905	0.406	1.000	0.000
3) IO018	44.094	0.563	0.750	0.661	0.666	2.376	0.545	0.406	0.395
4) 4145	29.417	0.885	0.874	0.976	0.000	2.062	0.264	0.900	0.486
5) 4124	28.905	1.000	0.959	0.652	1.841	1.861	1.000	0.909	0.730
6) 4166	84.966	1.000	1.000	1.000	0.000	1.000	1.000	1.000	0.639
7) IO008	51.888	0.538	0.623	0.627	5.312	1.946	0.121	0.679	0.367
8) IO001	45.379	1.000	0.882	0.800	0.978	1.622	1.000	0.909	0.836
9) 453	72.011	1.000	0.263	0.589	0.000	1.279	1.110	1.000	0.452

Table 2: Virtual resection metrics at which patients not actually rendered seizure free by surgery were predicted to be rendered seizure free by the virtual resection. Some patients did not achieve seizure freedom in the simulation (red). Abbreviations: SOZ: seizure onset zone; sim:simulation; RR:resection ration; FR; fast ripple: FRnet: FR network graph theoretical measure; percent_r: percent of the nodes in resection cavity included in virtual resection set; novel_r: percent of nodes in the resection set that were not in the resection cavity.

Patient	sim. Radius	SOZ RR	RonS RR	FRRR	spatial FRnet	temporal FRnet-A	temporal FRnet-B	percent_r	novel_r
10) IO005	29.848	0.818	0.821	0.776	0.000	2.222	0.207	0.600	0.800
11) IO012	18.417	1.000	0.879	0.737	3.083	4.898	0.084	0.818	0.471
12) 469	53.053	1.000	0.824	0.947	0.000	1.249	0.353	0.857	0.478
13) 4110	35.077	0.318	0.191	0.833	0.000	1.282	0.088	0.162	0.905
14) 462	75.660	1.000	0.906	0.429	4.360	0.894	0.262	1.000	0.600
15) IO023	74.120	1.000	0.935	0.942	0.000	1.206	0.096	0.000	1.000
16) IO013	85.596	1.000	0.769	0.814	2.517	1.076	1.000	1.000	0.832
17) IO015	50.239	0.625	0.992	0.915	3.261	1.629	0.099	0.000	1.000
18) IO018	64.902	1.000	0.998	0.932	2.602	1.001	1.000	1.000	0.589

medRxiv preprint doi: https://doi.org/10.1101/2024.03.26.24304802; this version posted May 4, 2024. The copyright holder for this preprint
(which was not certified by peer review) is the author/funder, who has granted medRxiv a license to display the preprint in perpetuity.
It is made available under a CC-BY 4.0 International license .

Figures

medRxiv preprint doi: https://doi.org/10.1101/2024.03.26.24304802; this version posted May 4, 2024. The copyright holder for this preprint
(which was not certified by peer review) is the author/funder, who has granted medRxiv a license to display the preprint in perpetuity.
It is made available under a CC-BY 4.0 International license .

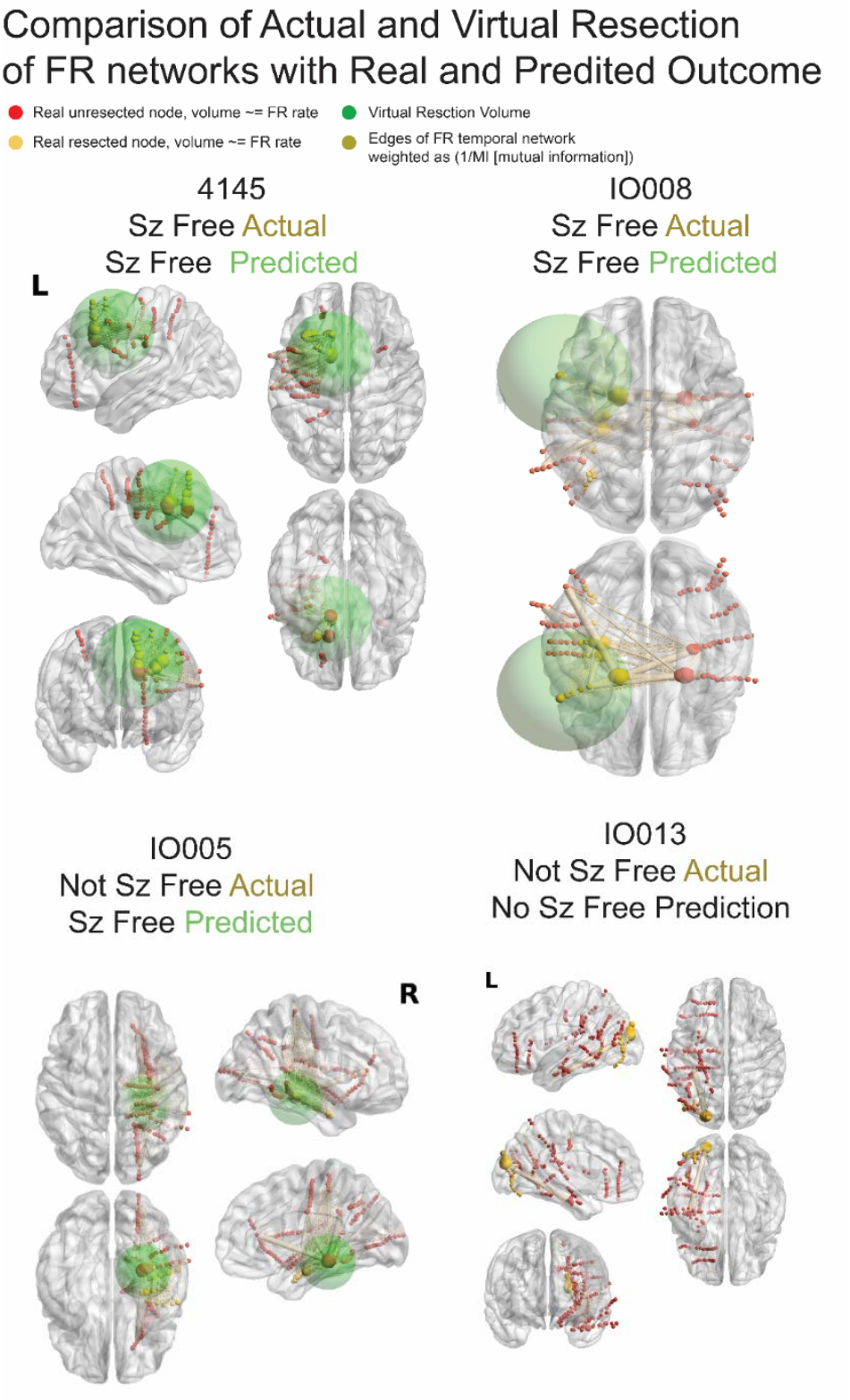

Figure 1: Illustration of fast ripple (FR) networks and real and simulated resections. In the four example patients, the sizes of red (unresected) and yellow (resected) nodes [i.e., stereo-EEG electrode contacts] are proportional to relative FR rate. The edges, connecting the nodes to one

medRxiv preprint doi: https://doi.org/10.1101/2024.03.26.24304802; this version posted May 4, 2024. The copyright holder for this preprint
(which was not certified by peer review) is the author/funder, who has granted medRxiv a license to display the preprint in perpetuity.
It is made available under a CC-BY 4.0 International license .

another, are weighted in size by the inverse of the mutual information (MI) of FR temporal correlations between the two nodes. In patients 4145 and IO008, who were actually rendered seizure free, the virtual resection overlaps strongly with the actually resected nodes. Also, the resection includes the nodes with the highest FR rates and connected by edges with the smallest MI. Patient IO005 was not actually rendered seizure free, the virtual resection that predicts seizure freedom is more posterior and includes nodes with high FR rate and low MI edges. Patient IO013 was also not rendered seizure free but the simulated virtual resection failed to achieve seizure freedom too.

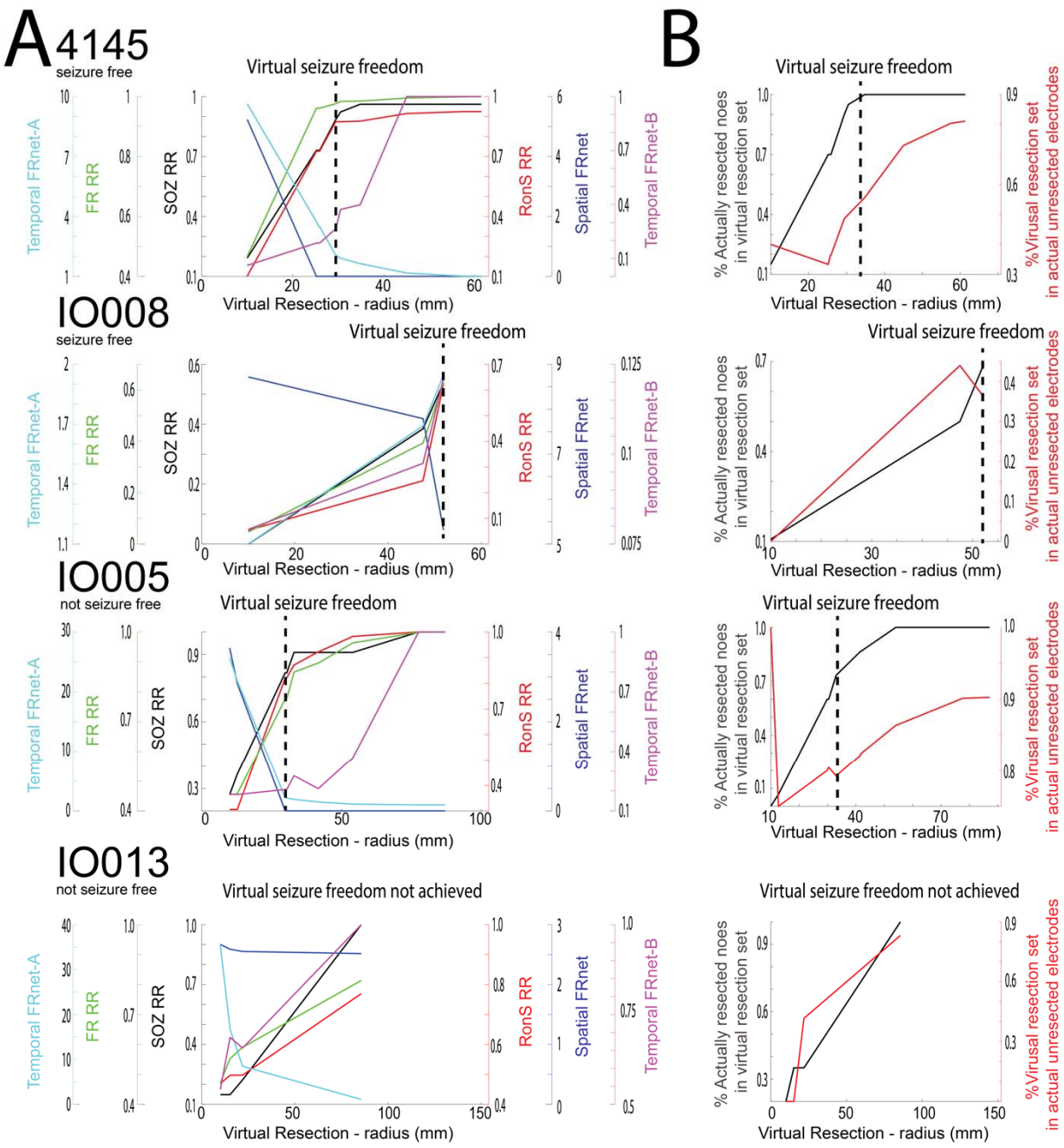

medRxiv preprint doi: https://doi.org/10.1101/2024.03.26.24304802; this version posted May 4, 2024. The copyright holder for this preprint
(which was not certified by peer review) is the author/funder, who has granted medRxiv a license to display the preprint in perpetuity.
It is made available under a CC-BY 4.0 International license .

Figure 2: Changes in resection metrics in individual patients at different resection volumes. A) Comparison of the seizure onset zone resection ratio (SOZ, RR), ripple on spike RR (RonS RR, red), fast ripple RR (FR RR, green), spatial FRnet (blue), temporal FRnet-A (cyan), temporal FRnet-B (magenta) for two seizure free example patients (top), and two non-seizure free example patients (bottom). The hashed vertical line indicates the iteration at which virtual seizure freedom is first achieved. Note that, among the metrics, only lower spatial FRnet-A values (blue) are intrinsically associated with seizure outcome. Temporal FRnet-A values less than 1 are associated with non-seizure freedom, but small resections of desynchronous high rate FR nodes can result in FRnet-A values >> 1. Among the four patients, only in IO013 did a simulated resection fail to result in a seizure free outcome. B) Corresponding plot of the percentage of actually resected nodes in the resection set (black), and percentage of the virtual resection set in actual unresected nodes (red) for each of the four patients.

medRxiv preprint doi: https://doi.org/10.1101/2024.03.26.24304802; this version posted May 4, 2024. The copyright holder for this preprint
(which was not certified by peer review) is the author/funder, who has granted medRxiv a license to display the preprint in perpetuity.
It is made available under a CC-BY 4.0 International license .

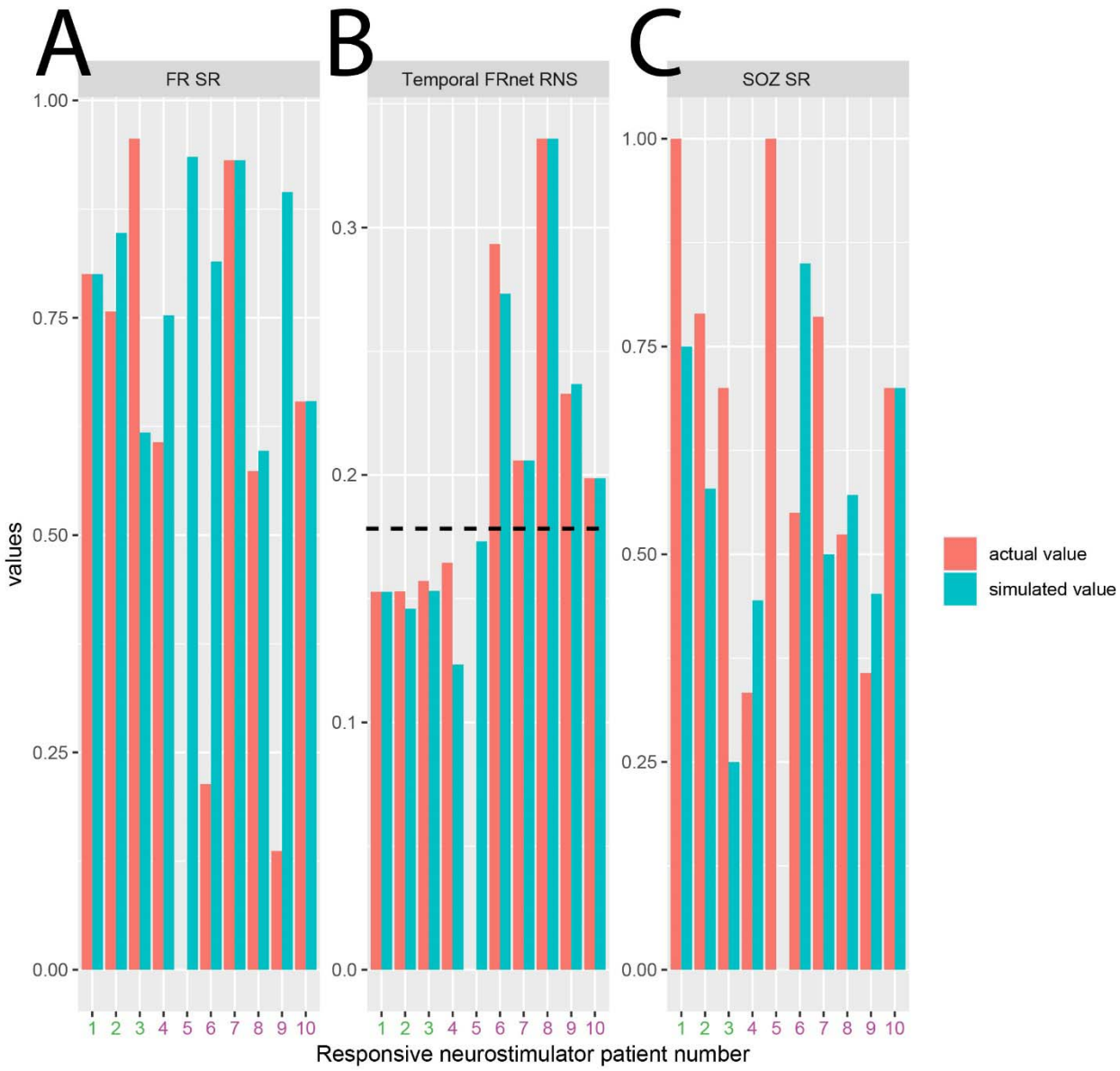

Figure 3: Simulated RNS lead placement and metrics that may predict RNS seizure outcome response. Fast ripple stimulation ratio (A, FR SR), temporal FRnet RNS (B, FR SGe), and SOZ stimulation ratio (C, SOZ SR) computed in patients 1-3 with a super responder outcome (green), and patients 4-10 with an intermediate responder outcome (magenta). In panel B note that patients 1-5 exhibited a simulated temporal FRnet RNS value less than patients 6-10 (horizontal hatched line). Placement of RNS leads in the simulated location thus may have resulted in five, rather than three, RNS super responder.

medRxiv preprint doi: https://doi.org/10.1101/2024.03.26.24304802; this version posted May 4, 2024. The copyright holder for this preprint
(which was not certified by peer review) is the author/funder, who has granted medRxiv a license to display the preprint in perpetuity.
It is made available under a CC-BY 4.0 International license .

1. Rosenow, F. & Lüders, H. Presurgical evaluation of epilepsy. *Brain* **124**, 1683–1700 (2001).

2. Jacobs, J. *et al.* High□frequency electroencephalographic oscillations correlate with outcome of epilepsy surgery. *Ann Neurol* **67**, 209–220 (2010).

3. Akiyama, T. *et al.* Focal resection of fast ripples on extraoperative intracranial EEG improves seizure outcome in pediatric epilepsy. *Epilepsia* **52**, 1802–1811 (2011).

4. Weiss, S. A. *et al.* Seizure localization using ictal phase-locked high gamma. *Neurology* **84**, 2320–2328 (2015).

5. Li, A. *et al.* Neural fragility as an EEG marker of the seizure onset zone. *Nat Neurosci* 1–10 (2021) doi:10.1038/s41593-021-00901-w.

6. Khan, M. *et al.* Proportion of resected seizure onset zone contacts in pediatric stereo-EEG-guided resective surgery does not correlate with outcome. *Clin Neurophysiol* **138**, 18–24 (2022).

7. Lin, J. *et al.* High frequency oscillation network dynamics predict outcome in non-palliative epilepsy surgery. *Brain Commun.* **6**, fcae032 (2024).

8. Téllez-Zenteno, J. F., Dhar, R. & Wiebe, S. Long-term seizure outcomes following epilepsy surgery: a systematic review and meta-analysis. *Brain* **128**, 1188–1198 (2005).

9. Engel, J. *et al.* Early Surgical Therapy for Drug-Resistant Temporal Lobe Epilepsy: A Randomized Trial. *Jama* **307**, 922–930 (2012).

10. Spencer, D. D., Gerrard, J. L. & Zaveri, H. P. The roles of surgery and technology in understanding focal epilepsy and its comorbidities. *Lancet Neurology* **17**, 373–382 (2018).

11. Frauscher, B. *et al.* High□frequency oscillations: The state of clinical research. *Epilepsia* **58**, 1316–1329 (2017).

12. Nevalainen, P. *et al.* Association of fast ripples on intracranial EEG and outcomes after epilepsy surgery. *Neurology* **95**, e2235–e2245 (2020).

13. Bragin, A., Wilson, C. L. & Engel, J. Chronic Epileptogenesis Requires Development of a Network of Pathologically Interconnected Neuron Clusters: A Hypothesis. *Epilepsia* **41**, S144–S152 (2000).

14. Bragin, A., Mody, I., Wilson, C. L. & Engel, J. Local Generation of Fast Ripples in Epileptic Brain. *J Neurosci* **22**, 2012–2021 (2002).

15. Li, L. *et al.* Spatial and temporal profile of high-frequency oscillations in posttraumatic epileptogenesis. *Neurobiol Dis* **161**, 105544 (2021).

16. Weiss, S. A. *et al.* Pathological neurons generate ripples at the UP-DOWN transition disrupting information transfer. (2023) doi:10.1101/2023.08.01.23293365.

medRxiv preprint doi: https://doi.org/10.1101/2024.03.26.24304802; this version posted May 4, 2024. The copyright holder for this preprint
(which was not certified by peer review) is the author/funder, who has granted medRxiv a license to display the preprint in perpetuity.
It is made available under a CC-BY 4.0 International license .

17. Bullmore, E. & Sporns, O. Complex brain networks: graph theoretical analysis of structural and functional systems. *Nat Rev Neurosci* **10**, 186–198 (2009).

18. Weiss, S. A. *et al.* Graph theoretical measures of fast ripples support the epileptic network hypothesis. *Brain Commun* (2022) doi:10.1093/braincomms/fcac101.

19. Weiss, S. A. *et al.* Graph theoretical measures of fast ripple networks improve the accuracy of post-operative seizure outcome prediction. *Sci. Rep.* **13**, 367 (2023).

20. Shi, W. *et al.* Spike ripples localize the epileptogenic zone best: an international intracranial study. *Brain* awae037 (2024) doi:10.1093/brain/awae037.

21. Weiss, S. A. *et al.* Stimulation better targets fast□ripple generating networks in super responders to the responsive neurostimulator system. *Epilepsia* (2023) doi:10.1111/epi.17582.

22. Plonsey, R. & Barr, R. C. *Bioelectricity A Quantitative Approach*. (Kluwer Academic/Plenum Publishers, 2000).

23. Ozen, S. *et al.* Transcranial electric stimulation entrains cortical neuronal populations in rats. *J Neurosci Official J Soc Neurosci* **30**, 11476–85 (2010).

24. Anastassiou, C. A., Perin, R., Markram, H. & Koch, C. Ephaptic coupling of cortical neurons. *Nat Neurosci* **14**, 217–223 (2011).

25. Radman, T., Su, Y., An, J. H., Parra, L. C. & Bikson, M. Spike Timing Amplifies the Effect of Electric Fields on Neurons: Implications for Endogenous Field Effects. *J Neurosci* **27**, 3030–3036 (2007).

26. Khambhati, A. N., Shafi, A., Rao, V. R. & Chang, E. F. Long-term brain network reorganization predicts responsive neurostimulation outcomes for focal epilepsy. *Sci Transl Med* **13**, eabf6588 (2021).

27. Avants, B. B., Epstein, C. L., Grossman, M. & Gee, J. C. Symmetric diffeomorphic image registration with cross-correlation: Evaluating automated labeling of elderly and neurodegenerative brain. *Med Image Anal* **12**, 26–41 (2008).

28. Desikan, R. S. *et al.* An automated labeling system for subdividing the human cerebral cortex on MRI scans into gyral based regions of interest. *Neuroimage* **31**, 968–980 (2006).

29. Waldman, Z. J. *et al.* A method for the topographical identification and quantification of high frequency oscillations in intracranial electroencephalography recordings. *Clin Neurophysiol* **129**, 308–318 (2018).

30. Weiss, S. A. *et al.* Accuracy of high-frequency oscillations recorded intraoperatively for classification of epileptogenic regions. *Sci Rep-uk* **11**, 21388 (2021).

31. Song, I. *et al.* Bimodal coupling of ripples and slower oscillations during sleep in patients with focal epilepsy. *Epilepsia* **58**, 1972–1984 (2017).

medRxiv preprint doi: https://doi.org/10.1101/2024.03.26.24304802; this version posted May 4, 2024. The copyright holder for this preprint
(which was not certified by peer review) is the author/funder, who has granted medRxiv a license to display the preprint in perpetuity.
It is made available under a CC-BY 4.0 International license .

32. Shimamoto, S. *et al.* Utilization of independent component analysis for accurate pathological ripple detection in intracranial EEG recordings recorded extra- and intra-operatively. *Clin Neurophysiol* **129**, 296–307 (2018).

33. Weiss, S. A. *et al.* Visually validated semi-automatic high-frequency oscillation detection aides the delineation of epileptogenic regions during intra-operative electrocorticography. *Clin Neurophysiol* **129**, 2089–2098 (2018).

34. Weiss, S. A. *et al.* Pathological neurons generate ripples at the UP□DOWN transition disrupting information transfer. *Epilepsia* **65**, 362–377 (2023).

35. Rubinov, M. & Sporns, O. Complex network measures of brain connectivity: Uses and interpretations. *Neuroimage* **52**, 1059–1069 (2010).

36. Gribkova, E. D., Ibrahim, B. A. & Llano, D. A. A novel mutual information estimator to measure spike train correlations in a model thalamocortical network. *J Neurophysiol* **120**, 2730–2744 (2018).

37. Guth, T. A. *et al.* Interictal spikes with and without high-frequency oscillation have different single-neuron correlates. *Brain* (2021) doi:10.1093/brain/awab288.

38. Weiss, S. A. *et al.* Fast ripples reflect increased excitability that primes epileptiform spikes. *Brain Commun.* fcad242 (2023) doi:10.1093/braincomms/fcad242.

39. Weiss, S. A. *et al.* Stimulation better targets fast ripple generating networks in super-responders to the responsive neurostimulator system (RNS). (2022) doi:10.1101/2022.11.30.22282937.

40. Weiss, S. A. *et al.* Delta oscillation coupled propagating fast ripples precede epileptiform discharges in patients with focal epilepsy. *Neurobiol Dis* 105928 (2022) doi:10.1016/j.nbd.2022.105928.

41. Bragin, A., Azizyan, A., Almajano, J., Wilson, C. L. & Engel, J. Analysis of Chronic Seizure Onsets after Intrahippocampal Kainic Acid Injection in Freely Moving Rats. *Epilepsia* **46**, 1592–1598 (2005).

42. Weiss, S. A. *et al.* Ictal onset patterns of local field potentials, high frequency oscillations, and unit activity in human mesial temporal lobe epilepsy. *Epilepsia* **57**, 111–121 (2016).

43. Otárula, K. A. G., Ellenrieder, N. von, Cuello□Oderiz, C., Dubeau, F. & Gotman, J. High□Frequency Oscillation Networks and Surgical Outcome in Adult Focal Epilepsy. *Ann Neurol* **85**, 485–494 (2019).